On the small divergence of laser-driven ion beams from nanometer thick foils

J. H. Bin, W. J. Ma, K. Allinger, H. Y. Wang, D. Kiefer et al.

Citation: Phys. Plasmas **20**, 073113 (2013); doi: 10.1063/1.4816031
View online: http://dx.doi.org/10.1063/1.4816031
View Table of Contents: http://pop.aip.org/resource/1/PHPAEN/v20/i7
Published by the AIP Publishing LLC.

On the small divergence of laser-driven ion beams from nanometer thick foils

J. H. Bin,[1,2] W. J. Ma,[1,2,a)] K. Allinger,[1,2] H. Y. Wang,[2,3] D. Kiefer,[1,2] S. Reinhardt,[1] P. Hilz,[1] K. Khrennikov,[1,2] S. Karsch,[1,2] X. Q. Yan,[3] F. Krausz,[1,2] T. Tajima,[1] D. Habs,[1,2] and J. Schreiber[1,2,b)]

[1]*Fakultät für Physik, Ludwig-Maximilians-Universität München, D-85748 Garching, Germany*
[2]*Max-Planck-Institut für Quantenoptik, D-85748 Garching, Germany*
[3]*State Key Laboratory of Nuclear Physics and Technology, and Key Lab of High Energy Density Physics Simulation, CAPT, Peking University, Beijing 100871, China*

(Received 7 May 2013; accepted 24 June 2013; published online 26 July 2013)

We report on experimental studies of divergence of proton beams from nanometer thick diamond-like carbon foils irradiated by a linearly polarized intense laser with high contrast. Proton beams with extremely small divergence (half angle) of 2° are observed in addition with a remarkably well-collimated feature over the whole energy range, showing one order of magnitude reduction of the divergence angle in comparison to the results from μm thick targets. Similar features are reproduced in two-dimensional particle-in-cell simulations with parameters representing our experiments, indicating a strong influence from the electron density distribution on the divergence of protons. Our comprehensive experimental study reveals grand opportunities for using nm foils in experiments that require high ion flux and small divergence. © *2013 AIP Publishing LLC*. [http://dx.doi.org/10.1063/1.4816031]

I. INTRODUCTION

The emission of highly energetic ions from solid targets irradiated by intense laser pulses has attracted great attention over the past decades.[1] The short time scale on which the acceleration occurs along with the small source size enable extremely high ion densities in the MeV bunches which could be superior for specific applications.[2–6] However, such high density is only maintained close to the source, it drops quickly due to the angular spread of few tens of degrees.[7,8] Such large angles lead to large losses using magnetic quadrupoles,[9] complicate the beam transport, and therefore trigger investigations on sophisticated transportation schemes such as pulsed solenoid[10] and laser driven micro lenses.[11] Meanwhile, shaped lens target,[12] droplets,[13] and curved target[14] have been used to manipulate the ions angular distribution. Experimental approaches were mostly based on target normal sheath acceleration (TNSA)[15] with μm thick targets. Acceleration fields are built at the target rear by the hot electrons generated at the front side of the targets. The divergence of the ions strongly depends on the electron density and phase space distribution of the electrons behind the target, which is initially related to the laser profile and then disturbed during the transportation through the targets.[16]

Recently, ultrathin foils with thickness down to nm scale have been investigated experimentally,[17–19] enabled by the improvement on the laser temporal contrast. A divergent ion beam with opening half angle of roughly 10° from 50 nm ultrathin foils can be inferred from Ref. 18. Proton beams with divergence of 5–6° have been observed from 800 nm CH targets.[19] These results imply that thinner foils can generate much more collimated ion emission as compared to μm thick targets.

In this paper, we present the first detailed study of the divergence of proton beams accelerated from 5–20 nm thick diamond-like-carbon (DLC) foils.[20] Divergences as low as 2° were observed for different target thickness and irradiation conditions. In comparison to μm thick targets, we observed more than 10 times reduction in the divergence. Meanwhile, the proton beams show a pronounced collimation over the whole energy range, which in our case reached up to 6 MeV. Two-dimensional (2D) particle-in-cell (PIC) simulations support our experimental findings and suggest that the small divergence is the result of a steep longitudinal electron density gradient that seems representative for nm thin foils. The constant divergence over the complete energy range maybe attributed to a transverse electron density distribution with similar function as in longitudinal. As none of the models for nm-foil ion acceleration[15,21–25] makes a prediction about the expected divergence, we give a simple explanation for the observation, consists with the simulation results.

II. EXPERIMENT

The experiments were performed with the ATLAS Ti:sapphire laser system at Max-Planck-Institute for Quantum Optics. This system delivers pulses with a duration of 30 fs full-width half-maximum (FWHM) centered at 795 nm wavelength. The laser polarization on the target is linear polarization. The initial laser contrast is 3×10^{-6} at 2 ps before the peak of main pulse. A re-collimating double plasma mirror system was introduced to further enhance the value to 10^{-9}. 400 mJ laser energy was delivered on target. A 90°$f/2$ off-axis parabolic mirror focuses the pulses to a measured FWHM diameter spot size of 3 μm, yielding peak intensity of 8×10^{19}W/cm^2. DLC foils of thickness 5, 10, and 20 nm have been irradiated under normal incidence for varying spot size, the actual spot size on target in the range of 3–19.2 μm has been adjusted by moving the target along the laser axis.

a)wenjun.ma@physik.uni-muenchen.de
b)joerg.schreiber@mpq.mpg.de

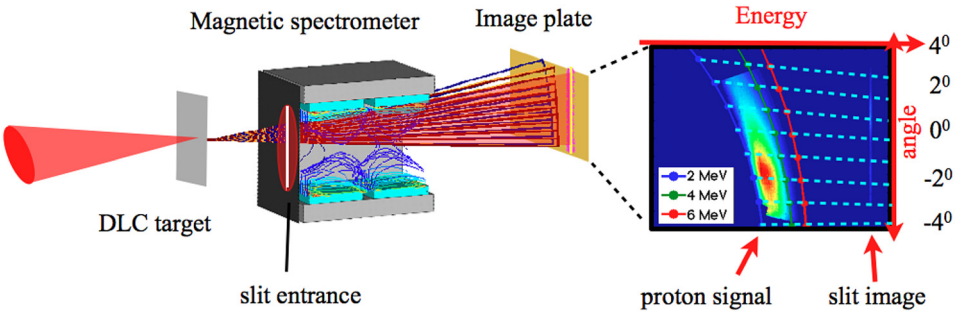

FIG. 1. Experimental setup. The divergence of protons characterized with the magnetic spectrometer and IP. The trajectory of protons through the magnetic field as well as the magnetic field structure is shown in the setup picture. The resulting isoenergy contours of the magnetic spectrometer are superimposed with a raw image of proton energy-angular distribution as it appears at the IP. The example is obtained with a 10 nm target displaced by 100 μm from the laser focal plane. The dashed lines in the inset indicate the different angles.

Fig. 1 shows the magnetic spectrometer with a gap of 14 cm employed for the proton beam measurements. A long vertical entrance slit of 300 μm width is placed in front of the magnetic field. This configuration enables angularly-resolved high-accuracy energy distribution measurement. Fujifilm BAS-TR image plates (IPs) were positioned at a distance of 30 cm behind the magnets to capture ion phase space over an angular range of 8°. The IPs have been absolutely calibrated at MLL Tandem accelerator.[26] A Layer of 45 μm Al foil was added in front of the IPs to block heavy ions and to protect IPs from direct and scattered laser light. Protons with energies beyond 2 MeV are recorded. A typical raw image from a 10 nm DLC foil is shown in Fig. 1. The modeled trajectory of proton beams through the dipole magnets as well as the magnetic field is shown in Fig. 1. The resultant isoenergy contours of the spectrometer shows how the proton propagates through the spectrometer and form a angular distribution on the detector. The image of the entrance slit, i.e., the zero line, and the low energy cutoff line from proton signal allows to extrapolate the average magnetic field for different angles, acting as a calibration process. The modeled 2 MeV isoenergy curve shows fair agreement of the experimental raw image for 2 MeV low energy cutoff by the Al foil after the calibration. Those isoenergy curves are used to transfer the two-dimensional spatial information from raw image to the energy angular distribution of protons. Throughout the experimental campaign, we observed exponentially decaying proton energy distributions with cut-off energy between 4 and 6 MeV.

The smallest divergence was observed with a 10 nm target displaced by 100 μm from the laser focal plane. Fig. 2(b) shows the energy-angular distribution of the example from Fig. 1 after normalization in order to highlight the collimation over the complete energy range. The divergence is almost constant over the detected energy range, resembling the aforementioned collimation. The angular distribution is fitted by a Gaussian function for each energy value. We define our divergence by the half value of FWHM of the fitting profile and plot these values as a function of proton energy normalized to the peak energy, as shown in Fig. 2(a) by the red curve. This enables a comparison to established results[7,8,10] which are represented in Fig. 2(a) as well. Compared to μm thick targets, the half angle from 10 nm foil is reduced by a factor of 10. Moreover, the typical increasing of divergence with decreasing energy is not observed. The results from experiment with 50 nm (Ref. 18) and 800 nm foils (Ref. 19) are included as well, indicating an overall reduction of divergence with decreasing target thickness.

Further on, the thickness of the targets and their positions with respect to the focal plane of the laser were varied. As shown above, the divergence showed no noticeable dependence on energy. Therefore, we plotted the average value of the half angle as a function of the target position in Fig. 3(a), the vertical error bar indicates the standard deviation for each shot while the horizontal error bar shows the positioning accuracy of about 10 μm, smaller than the Rayleigh length of 25 μm marked by the light blue area. The small divergence combined with the well-collimation feature is conserved during the whole parameter scan. The obtained divergences varied in the range of 2–4.6°, showing comparably small values. The divergence is maximized with a value of 4.6° in the focus plane for the thickest foil of 20 nm. For thinner foils (5 and 10 nm), these values are reduced to 3.3°, indicating a tendency of reducing divergence with decreasing of target thickness even in the nm scale. Moreover, the divergence of the protons decreases with increasing focal spot size on the target when moving the target out of focal plane to both sides beyond the Rayleigh length. The smallest divergence was obtained in the target position of +100 μm, which is our example of Fig. 2. The laser intensity distribution is single-peaked as shown for three exemplary

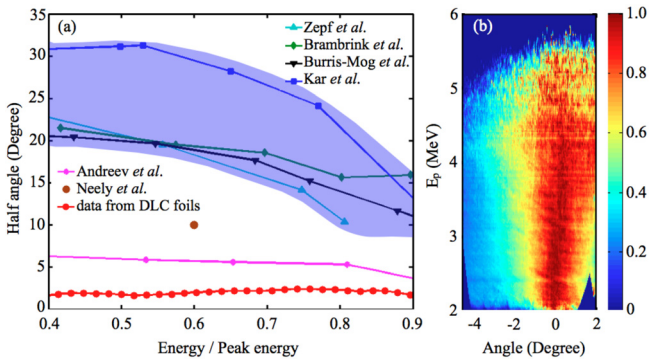

FIG. 2. (a) Beam divergence half angle as a function of proton energy for the most collimated beam from DLC foils, along with other data published in the literature from μm thick targets (the light blue area, presented by blue, green, black, and cyan curves)[7,8,10] and from nm scale thin targets (brown dot and magenta curve).[18,19] (b) Experimentally processed result of the data presented in Fig. 2(a) after normalization, where the color scale denotes the normalized fluence for given energy.

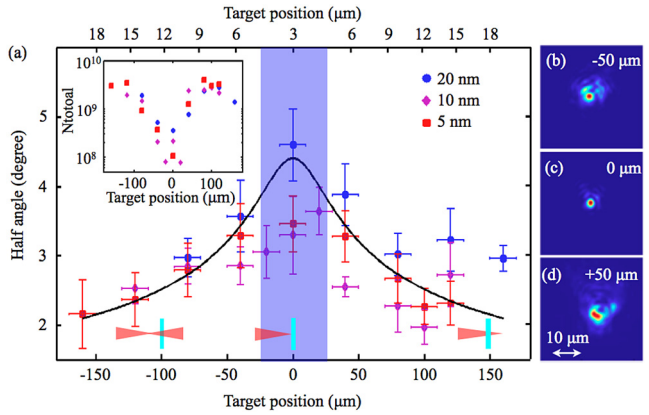

FIG. 3. (a) Beam divergence (half angle) for varying thickness of DLC foils and target positions. The lower axis shows the target position, where ± means the foils were placed before/after laser focal plane, as indicated by the small pictures. While the upper axis denotes the focal spot FWHM diameter D_L. The black curve is an empirical fitting curve showing the divergence scale with laser FWHM diameter $(D_L)^{-1/2}$. The inset presents the total number of protons for each shot. The Measured laser intensity distribution is shown at three target positions −50 μm (b), 0 μm (c), and 50 μm (d).

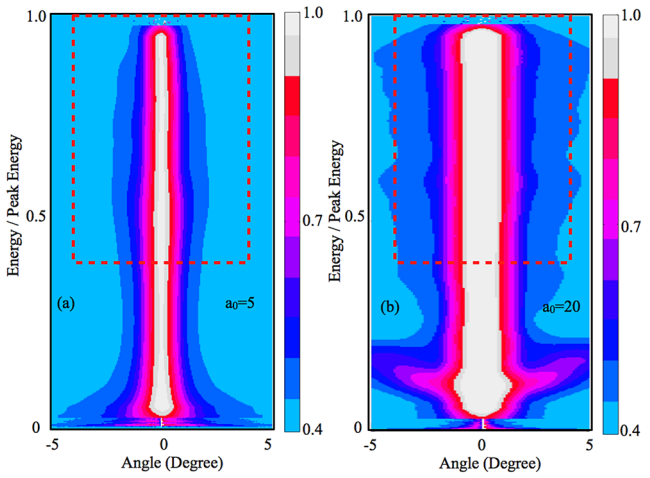

FIG. 4. Simulation result for proton angular distribution at $t = 100$ T after normalization with $a_0 = 5$ (a) and $a_0 = 20$ (b). Here T corresponds to one laser cycle, the red rectangles mark the experimental observation window. The targets are irradiated with the laser at the best focal position. The same color scale is used in both graph.

positions in Figs. 3(b)–3(d), which allows us defining a FWHM diameter D_L of the laser focal spot by fitting a Gaussian function. The measured D_L indeed scales as the classical prediction $D_L = D_{L0}\sqrt{1 + (z/z_R)^2}$ for different target positions with small deviation of <5%. Here, D_{L0} is the minimum FWHM diameter, z is the target position, and z_R is the Rayleigh length. An empirical scaling is found, showing that the divergence roughly scales with the laser FWHM diameter $(D_L)^{-1/2}$. Note that the maximum energy of protons is little influenced by the change of target position and varied between 4 and 6 MeV with the highest values preferably attained at ±100 μm, which is the same position for minimum divergence. In addition, the measured total number of protons above 2 MeV is extracted from the measured proton spectrum and corresponding divergence from the parameter scan, as shown in the inset of Fig. 3(a). Interestingly, it increases when enlarging the target positions, i.e., when the divergence reduces.

III. SIMULATION RESULTS OF ENERGY ANGULAR DISTRIBUTION

To get further qualitative insight, 2D PIC simulation was performed with the KLAP code.[21] Solid density ($n_0 = 350 n_c$, where n_c is the critical density) plasma slab was considered. The initial temperature of electrons is 1 keV. The simulation box is 60 λ in laser direction (x) and 20 λ in transverse direction (y) in 2D with a resolution of 200 cells/λ and 40 cells/λ, respectively. Each cell is filled with 400 quasiparticles. The spatial resolution and particle number are set to get sufficient resolution with a reasonable computational cost. A linearly polarized laser pulse with a Gaussian envelope in both the spatial and temporal distribution with a FWHM diameter D_L of 3 μm and a FWHM duration of 33 fs, is used to approximate the experiment conditions.

Fig. 4(a) shows the 2D simulation result of the energy-angular distribution of proton from a 40 nm foil with $a_0 = 5$ at the best focus position after normalization, proceeding in the same way as the experimental data. A well collimated proton beam is observed with a constant value of about 2° over the whole energy range, showing almost identical behaviors as the experimental observation [cf. Fig. 2(b)]. Further simulation was carried out with identical parameters except for a large $a_0 = 20$ as compared to our experimental condition with $a_0 = 5$. The simulation result is shown in Fig. 4(b). A larger divergence with a half angle value of about 4° is observed from simulation, which is a factor of two increases as compared with the simulated results with $a_0 = 5$ (see Fig. 4(a)). Still, the proton beam exhibits a well collimated feature under higher intensity. Those interesting features, the small divergence and the well collimation, seem representative for nm ultrathin foils in a larger range of variation on laser intensity. In addition, our simulation indicates that the divergence depends only weakly on the laser intensity with other parameters unchanged, i.e., $\theta \propto (I_0)^{1/4}$.

IV. DISCUSSION

Ion acceleration from nm thin foils has been discussed in a framework of many different mechanisms, including TNSA,[15] radiation pressure acceleration (RPA),[21,22] breakout afterburner (BOA),[23] light sail (LS),[24] and coherent acceleration of ions by laser (CAIL).[25] In our parameter, the coexistence of a number of these processes is likely.[27] More importantly, none of the existing models describes the divergence of the ions which is our main interest in this paper.

In a very simple picture, the divergence depends on the electric field direction during the acceleration phase. In turn, the electric field depends on the electron density distribution at a given time. Fig. 5(a) shows the longitudinal electron density distributions for the cases $a_0 = 5$ and $a_0 = 20$ at $t = 30$ T (when the laser pulse has just left the target) from our simulations. They are well represented by an exponential distribution with the longitudinal density scale length l_0 of 1/12 μm and 1/7 μm, respectively. Both values are much smaller than the typical values of few μm for μm targets.[28]

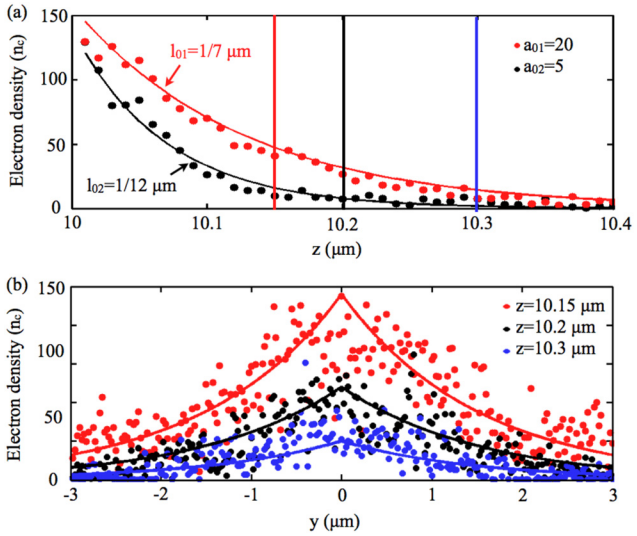

FIG. 5. (a) Longitudinal electron density distribution (z axis) at $y = 0$ at $t = 30\,\mathrm{T}$ with laser intensities $a_{01} = 20$ (red) and $a_{02} = 5$ (black), respectively. The targets were initially located at $z = 10\,\mu\mathrm{m}$. The dots denote the simulated results while the curves are the fitting functions. (b) Transverse electron density distribution (y axis) at three different z positions with $a_{02} = 5$ (as denoted by different color lines in (a)). The transverse density profiles are fitted by an exponential function with a scale length $l_y = 1.5\,\mu\mathrm{m}$.

And l_0 increases roughly by a factor of 2 owing to the higher electron temperature under higher laser intensity, consistent with the increase in the divergence of protons (see Fig. 4).

It is this steep longitudinal electron density gradient which tears the acceleration field forward, i.e., reduces the divergence with deceasing target thickness from μm to nm, which can be understood by the following simple picture. We assume that the local electric field direction is defined as $\alpha = E_y/E_z$, where y and z are the transversal and the longitudinal dimension, respectively. With an exponential distribution of the electrons, one derives the emission angle of protons θ as

$$\theta = \arctan\left(\int_0^\infty \alpha E_z dt \Big/ \int_0^\infty E_z dt\right) \approx \arctan\langle\alpha\rangle, \\ = \arctan\left\langle \frac{\partial n_e}{\partial y} \Big/ \frac{\partial n_e}{\partial z} \right\rangle, \quad (1)$$

where n_e is the electron density and the angle bracket denotes the average along the ion trajectory. Obviously, the larger the longitudinal density gradient (i.e., the smaller the scale length), the smaller the angle of divergence θ.

Moreover, Eq. (1) predicts the influence of transverse electron density on the divergence of ions as well, similar to Ref. 16. It could even explain the independence of divergence on the energy of protons in our experiments, if we assume that the transverse electron density distribution has the same functional dependency as the longitudinal one, i.e., exponential. As one can see from Fig. 5(b), the results from PIC results are not contradicting this hypothesis. With the transverse scale length l_y obtained from our fitting curves, a constant value of $\theta \propto \arctan(l_0/l_y) \sim 3.2°$, independent on the energy and the trajectory of ions, is obtained.

V. CONCLUSION

In conclusion, we investigated the divergence of proton beams generated from ultrathin DLC foils in detail. We demonstrated experimentally well collimated proton beams with divergence half angle as low as 2°. This constitutes the smallest value reported so far and one order of magnitude lower than achieved with μm targets. As a consequence, 100 times increase in proton fluence is observed.[29] Moreover, the proton beams are well-collimated over the complete energy range and can be further optimized by adjusting the focal spot size. Our study substantially extends the parameter range studied so far.[18,19] The obtained experimental results indicate a reduction of divergence with foil thickness in the nm-range. Understanding the exact mechanisms responsible for this beneficial behavior motivates future investigation. We expect these observations to be of particularly interest for applications. For example, investigations on the fundamental research in warm dense matter which request an intense and short ion bunch to heat solid dense material,[14,30] can benefit from high flux due to the small divergence. The high flux could also be beneficial to fast ignition[2] and neutron generation.[31] Furthermore, a small angle of divergence relaxes the requirement of beam transportation which is essential in specific applications of ions, for example, ion cancer therapy.[3]

ACKNOWLEDGMENTS

This work was supported by DFG through Transregio SFB TR18 and the DFG Cluster of Excellence Munich Centre for Advanced Photonics (MAP). J. H. Bin and D. Kiefer acknowledge financial support from IMPRS-APS.

[1]A. Maksimchuk, S. Gu, K. Flippo, D. Umstadter, and V. Yu. Bychenkov, Phys. Rev. Lett. **84**, 4108 (2000); E. L. Clark, K. Krushelnick, M. Zepf, F. N. Beg, M. Tatarakis, A. Machacek, M. I. K. Santala, P. A. Norreys, and A. E. Dangor, *ibid.* **85**, 1654 (2000); R. A. Snavely, M. H. Key, S. P. Hatchett, T. E. Cowan, M. Roth, T. W. Phillips, M. A. Stoyer, E. A. Henry, T. C. Sangster, M. S. Singh, S. C. Wilks, A. MacKinnon, A. Offenberger, D. M. Pennington, K. Yasuike, A. B. Langdon, B. F. Lasinski, J. Johnson, M. D. Perry, and E. M. Campbell, *ibid.* **85**, 2945 (2000); S. P. Hatchett, C. G. Brown, T. E. Cowan, E. A. Henry, J. S. Johnson, M. H. Key, J. A. Koch, A. B. Langdon, B. F. Singh, R. A. Snavely, M. A. Stoyer, S. C. Wilks, and K. Yasuike, Phys. Plasmas **7**, 2076 (2000); H. Daido, M. Nishiuchi, and A. S. Pirozhkov, Rep. Prog. Phys. **75**, 056401 (2012), and references therein.
[2]M. Roth, T. E. Cowan, M. H. Key, S. P. Hatchett, C. Brown, W. Fountain, J. Johnson, D. M. Pennington, R. A. Snavely, S. C. Wilks, K. Yasuike, H. Ruhl, F. Pegoraro, S. V. Bulanov, E. M. Campbell, M. D. Perry, and H. Powell, Phys. Rev. Lett. **86**, 436 (2001).
[3]V. Malka, S. Fritzler, E. Lefebvre, E. d'Humieres, R. Ferrand, G. Grillon, C. Albaret, S. Meyroneinc, J. Chambaret, A. Antonetti, and D. Hulin, Med. Phys. **31**, 1587 (2004).
[4]K. Krushelnik, E. L. Clark, R. Allott, F. N. Beg, C. N. Danson, A. Machacek, V. Malka, Z. Najmudin, D. Neely, P. A. Norreys, M. R. Salvati, M. I. K. Santala, M. Tatarakis, I. Watts, M. Zepf, and A. E. Dangor, IEEE Trans. Plasma Sci. **28**, 1110 (2000).
[5]J. A. Cobble, R. P. Johnson, T. E. Cowan, N. Renard-Le Galloudec, and M. Allen, J. Appl. Phys. **92**, 1775 (2002).
[6]D. Habs, T. Tajima, J. Schreiber, C. P. J. Barty, M. Fujiwara, and P. G. Thirolf, Eur. Phys. J. D **55**, 279 (2009).
[7]M. Zepf, E. L. Clark, F. N. Beg, R. J. Clarke, A. E. Dangor, A. Gopal, K. Krushelnick, P. A. Norreys, M. Tatarakis, U. Wagner, and M. S. Wei, Phys. Rev. Lett. **90**, 064801 (2003); E. Brambrink, J. Schreiber, T. Schlegel, P. Audebert, J. Cobble, J. Fuchs, M. Hegelich, and M. Roth, *ibid.* **96**, 154801 (2006).

[8]S. Kar, K. Markey, M. Borghesi, D. C. Carroll, P. McKenna, D. Neely, M. N. Quinn, and M. Zepf, Phys. Rev. Lett. **106**, 225003 (2011).
[9]M. Schollmeier, S. Becker, M. Geissel, K. A. Flippo. A. Blazevic, S. A. Gaillard, D. C. Gautier, F. Gruener, K. Harres, M. Kimmel, F. Nuernberg, P. Rambo, U. Schramm, J. Schreiber, J. Schuetrumpf, J. Schwarz, N. A. Tahir, B. Atherton, D. Habs, B. M. Hegelich, and M. Roth, Phys. Rev. Lett. **101**, 055004 (2008).
[10]T. Burris-Mog, K. Harres, F. Nuernberg, S. Busold, M. Bussmann, O. Deppert, G. Hoffmeister, M. Joost, M. Sobiella, A. Tauschwitz, B. Zielbauer, V. Bagnoud, T. Herrmannsdoerfer, M. Roth, and T. E. Cowan, Phys. Rev. ST Accel. Beams **14**, 121301 (2011).
[11]T. Toncian, M. Borghesi, J. Fuchs, E. d'Humieres, P. Antici, P. Audebert, E. Brambrink, C. A. Cecchetti, A. Pipahl, L. Romagnani, and O. Willi, Science **312**, 410 (2006).
[12]S. Kar, K. Markey, P. T. Simpson, C. Bellei, J. S. Green, S. R. Nagel, S. Kneip, D. C. Carroll, B. Dromey, L. Willingale, E. L. Clark, P. McKenna, Z. Najmudin, K. Krushelnick, P. Norreys, R. J. Clarke, D. Neely, M. Borghesi, and M. Zepf, Phys. Rev. Lett. **100**, 105004 (2008).
[13]T. Sokollik, M. Schnuerer, S. Steinke, P. V. Nickles, W. Sandner, M. Amin, T. Toncian, O. Willi, and A. A. Andreev, Phys. Rev. Lett. **103**, 135003 (2009).
[14]P. K. Patel, A. J. Mackinnon, M. H. Key, T. E. Cowan, M. E. Foord, M. Allen, D. F. Price, H. Ruhl, P. T. Springer, and R. Stephens, Phys. Rev. Lett. **91**, 125004 (2003).
[15]S. C. Wilks, A. B. Langdon, T. E. Cowan, M. Roth, M. Singh, S. Hatchett, M. H. Key, D. Pennington, A. MacKinnon, and R. A. Snavely, Phys. Plasmas **8**, 542 (2001).
[16]J. Fuchs, T. E. Cowan, P. Audebert, H. Ruhl, L. Gremillet, A. Kemp, M. Allen, A. Blazevic, J.-C. Gauthier, M. Geissel, M. Hegelich, S. Karsch, P. Parks, M. Roth, Y. Sentoku, R. Stephens, and E. M. Campbell, Phys. Rev. Lett. **91**, 255002 (2003); M. Schollmeier, K. Harres, F. Nuernberg, A. Blazevic, P. Audebert, E. Brambrink, J. C. Fernandez, K. A. Flippo, D. C. Gautier, M. Geissel, B. M. Hegelich, J. Schreiber, and M. Roth, Phys. Plasmas **15**, 053101 (2008). K. Zeil, J. Metzkes, T. Kluge, M. Bussmann, T. E. Cowan, S. D. Kraft, R. Sauerbrey, and U. Schramm, Nat. Commun. **3**, 874 (2012).
[17]A. Henig, D. Kiefer, K. Markey, D. C. Gautier, K. A. Flippo, S. Letzring, R. P. Johnson, T. Shimada, L. Yin, B. J. Albright, K. H. Bowers, J. C. Fernandez, S. G. Rykovanov, H.-C. Wu, M. Zepf, D. Jung, V. Kh. Liechtenstein, J. Schreiber, D. Habs, and B. M. Hegelich, Phys. Rev. Lett. **103**, 045002 (2009); A. Henig, S. Steinke, M. Schnuerer, T. Sokollik, R. Hoerlein, D. Kiefer, D. Jung, J. Schreiber, B. M. Hegelich, X. Q. Yan, J. Meyer-ter-Vehn, T. Tajima, P. V. Nickles, W. Sandner, and D. Habs, *ibid.* **103**, 245003 (2009); S. Steinke, A. Henig, M. Schnuerer, T. Sokollik, P. V. Nickles, D. Jung, D. Kiefer, R. Hoerlein, J. Schreiber, T. Tajima, X. Q. Yan, M. Hegelich, J. Meyer-ter-Vehn, W. Sandner, and D. Habs, Laser Part. Beams **28**, 215 (2010).
[18]D. Neely, P. Foster, A. Robinson, F. Lindau, O. Lundh, A. Persson, C.-G. Wahlstroem, and P. McKenna, Appl. Phys. Lett. **89**, 021502 (2006).
[19]A. Andreev, T. Ceccotti, A. Levy, K. Platonov, and Ph. Martin, New J. Phys. **12**, 045007 (2010).
[20]W. Ma, V. Kh. Liechtenstein, J. Szerypo, D. Jung, P. Hilz, B. M. Hegelich, H. J. Maier, J. Schreiber, and D. Habs, Nucl. Instr. Methods Phys. Res. A **655**, 53 (2011).
[21]X. Q. Yan, C. Lin, Z. M. Sheng, Z. Y. Guo, B. C. Liu, Y. R. Lu, J. X. Fang, and J. E. Chen, Phys. Rev. Lett. **100**, 135003 (2008).
[22]A. Macchi, F. Cattani, T. V. Liseykina, and F. Cornolti, Phys. Rev. Lett. **94**, 165003 (2005); A. P. L. Robinson, P. Gibbon, M. Zepf, S. Kar, R. G. Evans, and C. Bellei, Plasma Phys. Controlled Fusion **51**, 024004 (2009).
[23]L. Yin, B. J. Albright, B. M. Hegelich, and J. C. Fernandez, Laser Part. Beams **24**, 291 (2006); L. Yin, B. J. Albright, B. M. Hegelich, K. J. Bowers, K. A. Flippo, T. J. T. Kwan, and J. C. Fernandez, Phys. Plasmas **14**, 056706 (2007); L. Yin, B. J. Albright, K. J. Bowers, D. Jung, J. C. Fernandez, and B. M. Hegelich, Phys. Rev. Lett. **107**, 045003 (2011).
[24]J. F. L. Simmons and C. R. McInnes, Am. J. Phys. **61**, 205 (1993); B. Qiao, M. Zepf, M. Borghesi, and M. Geissler, Phys. Rev. Lett. **102**, 145002 (2009); A. Macchi, S. Veghini, and F. Pegoraro, *ibid.* **103**, 085003 (2009); B. Qiao, M. Zepf, M. Borghesi, B. Dromey, M. Geissler, A. Karmakar, and P. Gibbon, *ibid.* **105**, 155002 (2010).
[25]T. Tajima, D. Habs, and X. Q. Yan, Rev. Accel. Sci. Tech. **2**, 201 (2009).
[26]S. Reinhardt, Ph. D. thesis, Ludwig-Maximilians-Universität München, Munich, 2012.
[27]A. A. Andreev, S. Steinke, M. Schnuerer, A. Henig, P. V. Nickles, K. Y. Platonov, T. Sokollik, and W. Sandner, Phys. Plasmas **17**, 123111 (2010); A. A. Andreev, K. Yu. Platonov, M. Schnuerer, R. Prasad, and S. Ter-Avetisyan, Phys. Plasmas **20**, 033110 (2013).
[28]A. J. Mackinnon, M. Borghesi, S. Hatchett, M. H. Key, P. K. Patel, H. Campbell, A. Schiavi, R. Snavely, S. C. Wilks, and O. Willi, Phys. Rev. Lett. **86**, 1769 (2001); O. Jäckel, J. Polz, S. M. Pfotenhauer, H.-P. Schlenvoigt, H. Schwoerer, and M. C. Kaluza, New J. Phys. **12**, 103027 (2010); J. Fuchs, C. A. Cecchetti, M. Borghesi, T. Grismayer, E. d'Humieres, P. Antici, S. Atzeni, P. Mora, A. Pipahl, L. Romagnani, A. Schiaiv, Y. Sentoku, T. Toncian, P. Audebert, and O. Willi, Phys. Rev. Lett. **99**, 015002 (2007).
[29]J. Bin, K. Allinger, W. Assmann, G. Dollinger, G. A. Drexler, A. A. Friedl, D. Habs, P. Hilz, R. Hoerlein, N. Humble, S. Karsch, K. Khrennikov, D. Kiefer, F. Krausz, W. Ma, D. Michalski, M. Molls, S. Raith, S. Reinhardt, B. Roeper, T. E. Schmid, T. Tajima, J. Wenz, O. Zlobinskaya, J. Schreiber, and J. J. Wilkens, Appl. Phys. Lett. **101**, 243701 (2012).
[30]G. M. Dyer, A. C. Bernstein, B. I. Cho, J. Osterholz, W. Grigsby, A. Dalton, R. Shepherd, Y. Ping, H. Chen, K. Widmann, and T. Ditmire, Phys. Rev. Lett. **101**, 015002 (2008).
[31]M. Roth, D. Jung, K. Falk, N. Guler, O. Deppert, M. Devin, A. Favalli, J. Fernandez, D. Gautier, M. Geissel, R. Haight, C. E. Hamilton, B. M. Hegelich, R. P. Johnson, F. Merrill, G. Schaumann, K. Scheenberg, K. Schollmeier, T. Shimada, T. Taddeucci, J. L. Tybo, F. Wagner, S. A. Wender, C. H. Wilde, and G. A. Wurden, Phys. Rev. Lett. **110**, 044802 (2013).